Supporting Information for:

Post-Synthesis Boron-Doping of Silicon Quantum dot via Hydrogen Silsesquioxane-Capped Thermal Diffusion

Sarah Milliken, I Teng Cheong, Kai Cui, Jonathan G.C. Veinot

Table of Contents:

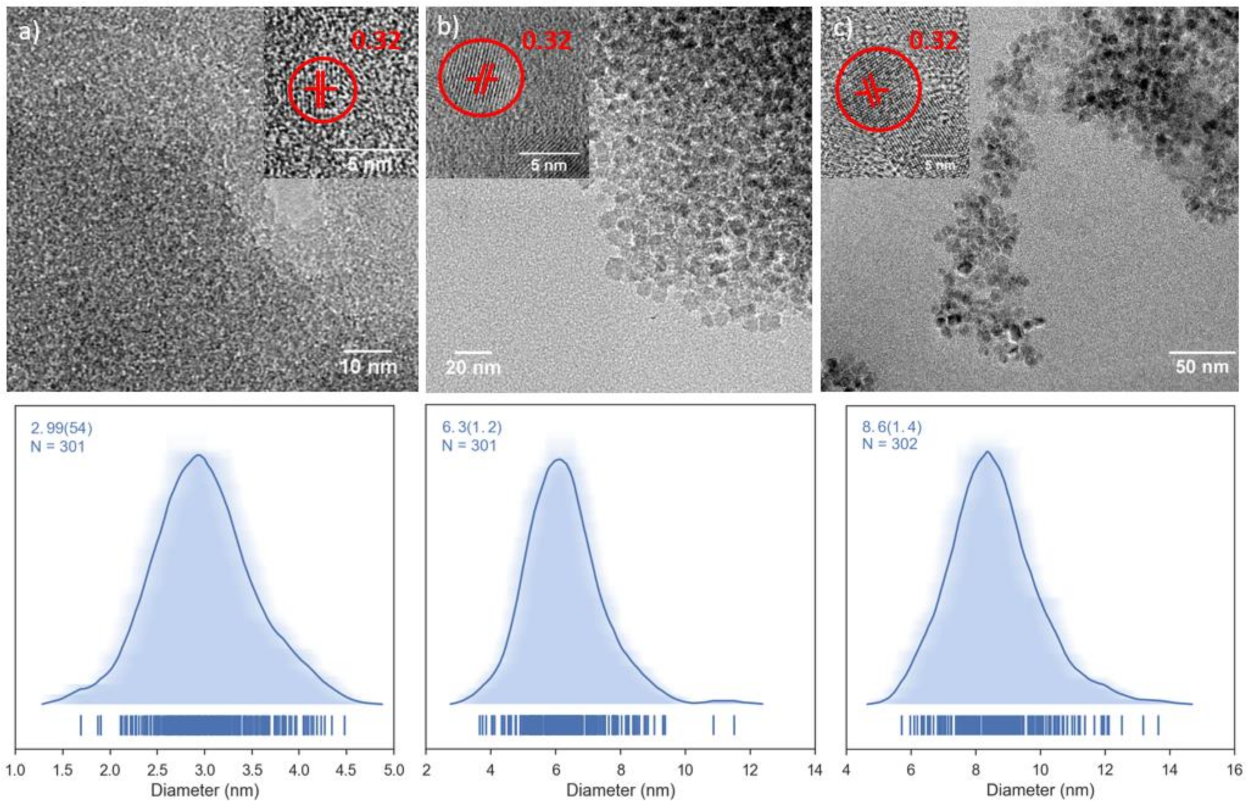

Figure S1 Bright field transmission electron microscopy (TEM), corresponding histograms, and high-resolution (inset) imaging showing fringes separated by 0.32 nm characteristic of the (111) lattice spacing of crystalline Si. a) 2.99 ± 0.54 nm b) 6.30 ± 1.2 nm and c) 8.60 ± 1.4 nm.

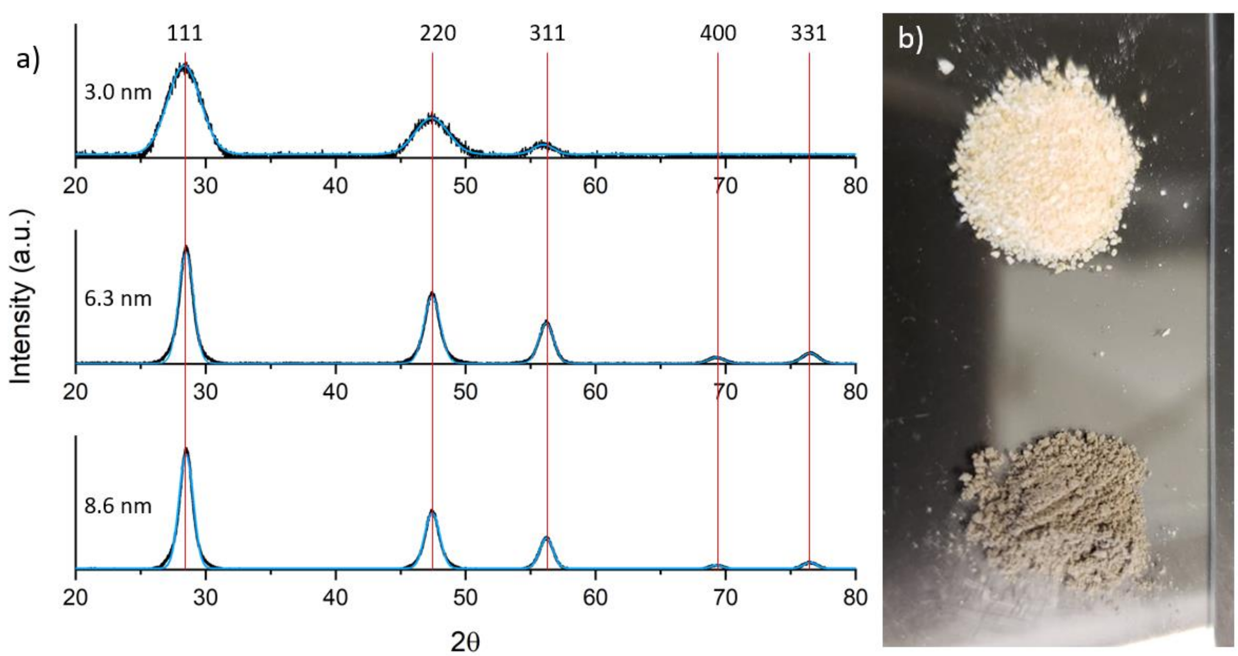

Figure S2 a) Powder X-ray diffraction patterns obtained from the precursor intrinsic SiQDs bearing TEM determined particle sizes of 2.99 ± 0.54 nm, 6.30 ± 1.2 nm and 8.60 ± 1.4 nm. Each pattern shows broadened reflections characteristic Si 111, 220, 311, 400 and 331. Experimental data is shown as black traces. Blue traces show the Gaussian-Lorentzian multiple-peak fitting. b) A representative photograph showing a reaction mixture containing SiQDs, boric acid and HSQ before (top) and after (bottom) drive-in annealing.

Crystallite size calculations:

The average crystallite size was calculated from the FWHM of the Gaussian-Lorentzian fit for reflections corresponding to the cubic crystalline Si in the PXRD patterns of the precursor and B-doped SiQDs (Figure S2 and Figure S8) using the following equation:

$$D = \frac{\kappa\lambda}{\beta cos\theta}$$

Where,

D = crystallite size (nm)

κ = 0.9 (Scherrer constant)

λ = 0.15406 nm (X-ray source wavelength)

β = FWHM (radians)

θ = peak position (radians)

Table S1: Debye-Scherrer analysis of powder X-ray diffraction patterns collected from preformed intrinsic SiQDs of TEM determined sizes: 2.99 ± 0.54 nm, 6.30 ± 1.2 nm and 8.60 ± 1.4 nm.

d_{TEM} = 2.99 nm			d_{TEM} = 6.30 nm			d_{TEM} = 8.60 nm		
Peak position (2θ)	**FWHM**	**Crystallite Size (nm)**	**Peak position (2θ)**	**FWHM**	**Crystallite Size (nm)**	**Peak position (2θ)**	**FWHM**	**Crystallite Size (nm)**
28.40	4.40	1.88	28.50	2.33	3.52	28.50	1.28	6.40
47.43	3.61	2.40	47.42	2.45	3.54	47.42	1.35	6.41
56.13	3.39	2.65	56.20	2.33	3.86	56.20	1.21	7.43

Table S2: Measured weight-loss of the HSQ/Boric acid/SiQD composites pre- and post-anneal for temperatures of 400 – 600 °C using Ar or 5:95 H_2:Ar atmosphere.

Temperature (°C)	Annealing Atmosphere	Weight-loss
Pre-anneal	N/A	19.71
400	Ar	14.44
500	Ar	5.80
600	Ar	4.47
400	5:95 H_2:Ar	7.96
500	5:95 H_2:Ar	4.45
600	5:95 H_2:Ar	3.80

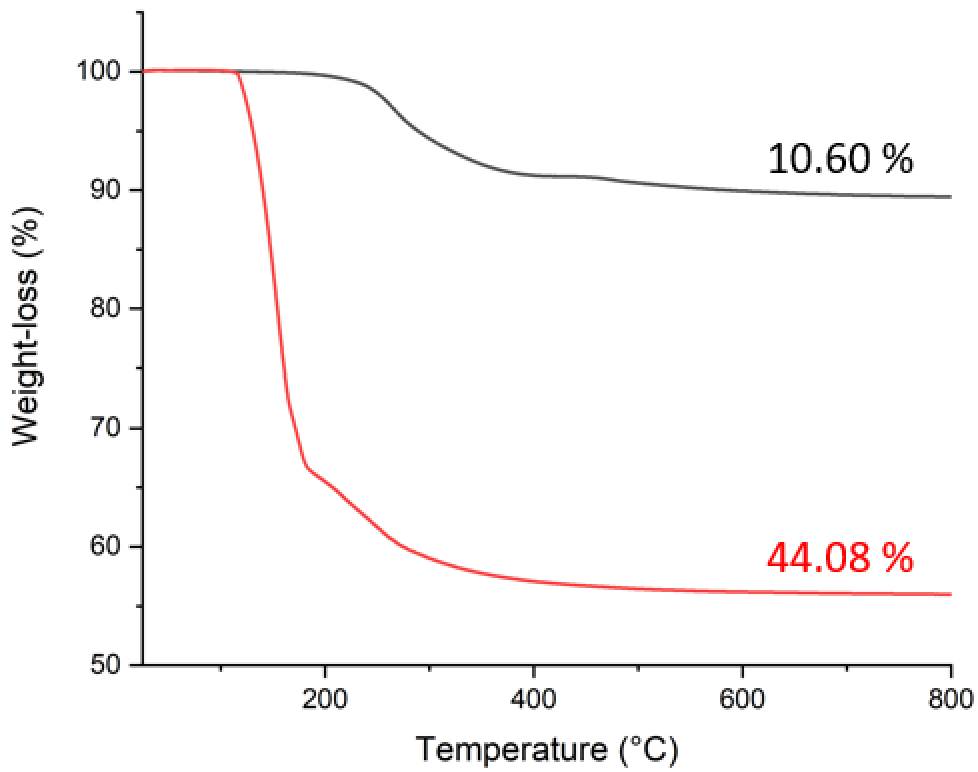

Figure S3 Thermomgravimetric analysis of boric acid (dopant precursor; red curve) and hydrogen silsesquioxane (HSQ; capping agent; black curve)

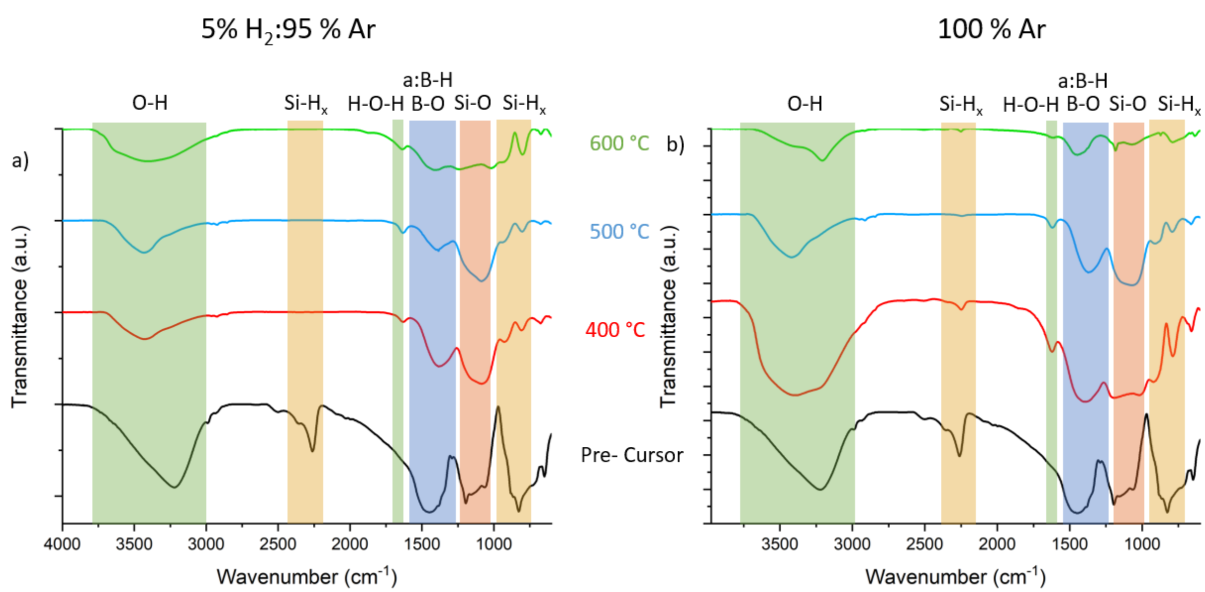

Figure S4 FTIR of the HSQ/Boric acid/SiQD precursor mixture and the corresponding composites produced after annealing at indicated temperatures using an atmosphere of a) 5 % H_2 :95 % Ar or b) Ar

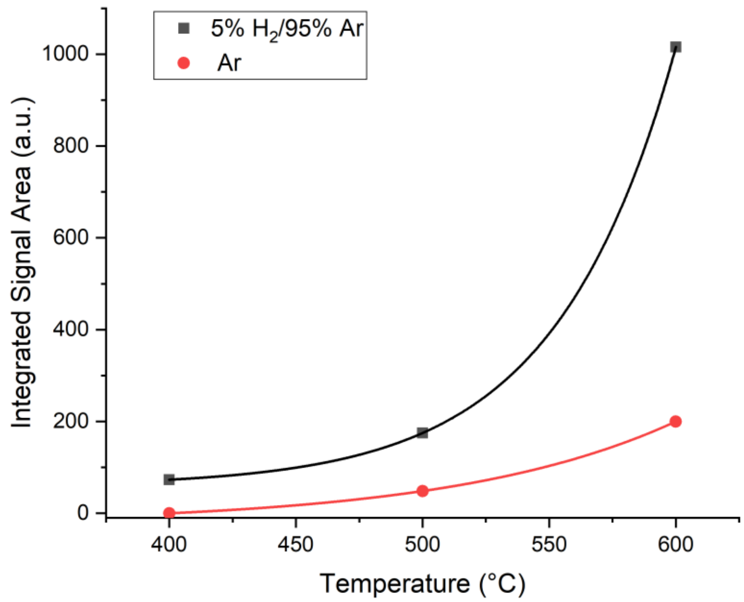

Figure S5 Integrated area of signal in the B 1s XP spectra for composites produced after annealing at temperatures of 400 – 600 °C using an atmosphere of Ar (red curve) or 5 % H_2 : 95 % Ar (black curve).

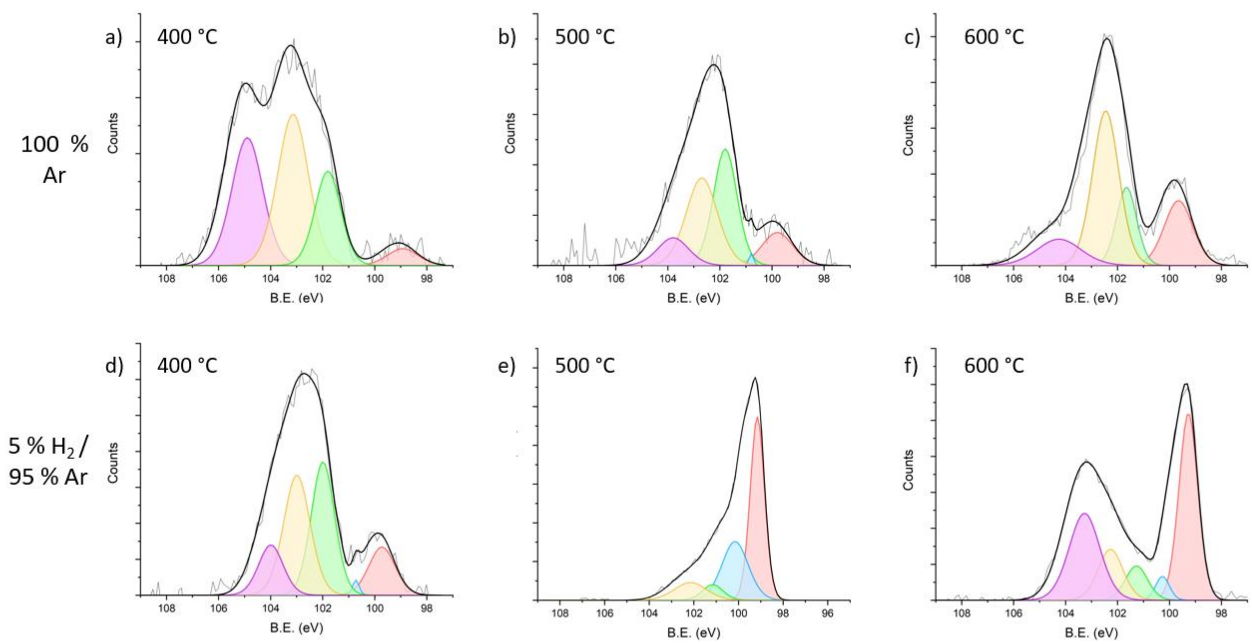

Figure S6 High-resolution Si 2p XP spectra of B-doped SiQDs obtained from annealing precursor particles in flowing Ar and 5:95 H_2:Ar atmospheres at indicated temperatures.

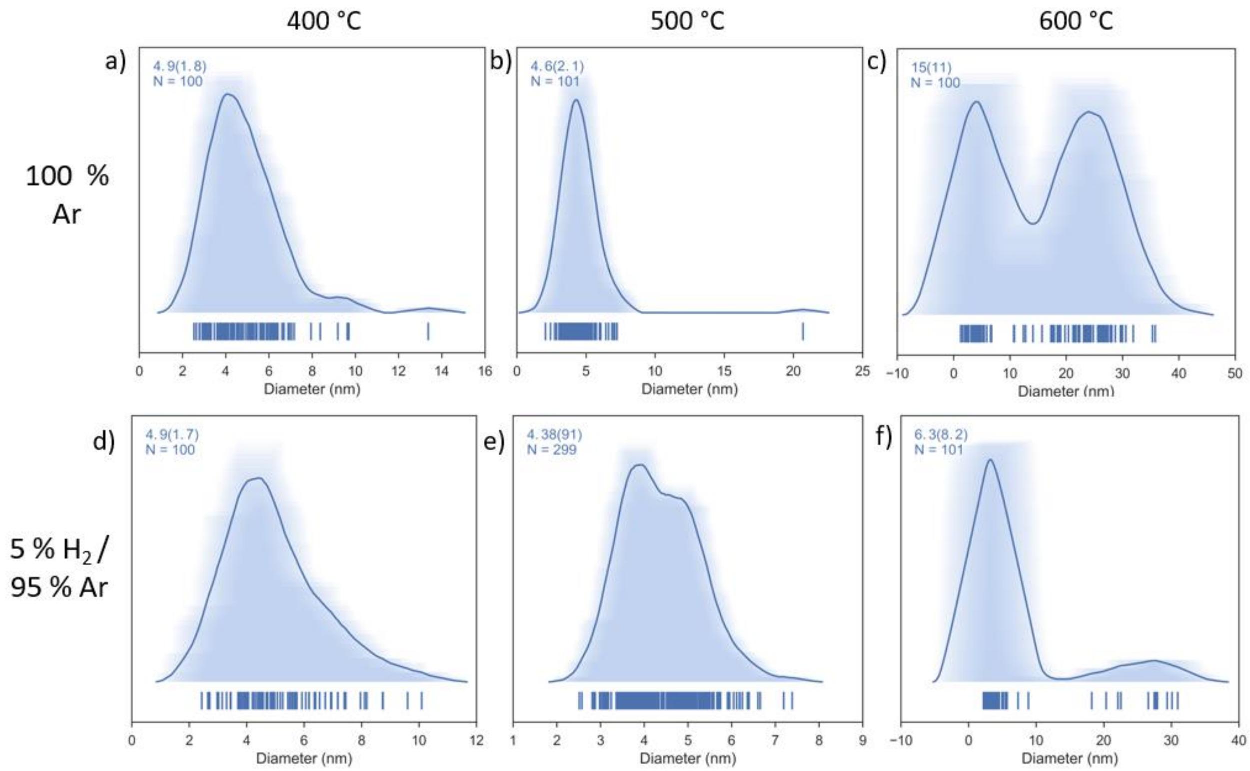

Figure S7 Average shifted histograms of particle sizes obtained from bright field TEM images of B-doped SiQDs obtained from composites annealed in Ar at a) 400 °C, b) 500 °C, c) 600 °C and 5:95 H_2:Ar at d) 400 °C, e) 500 °C, f) 600 °C. N represents the number of particles measured.

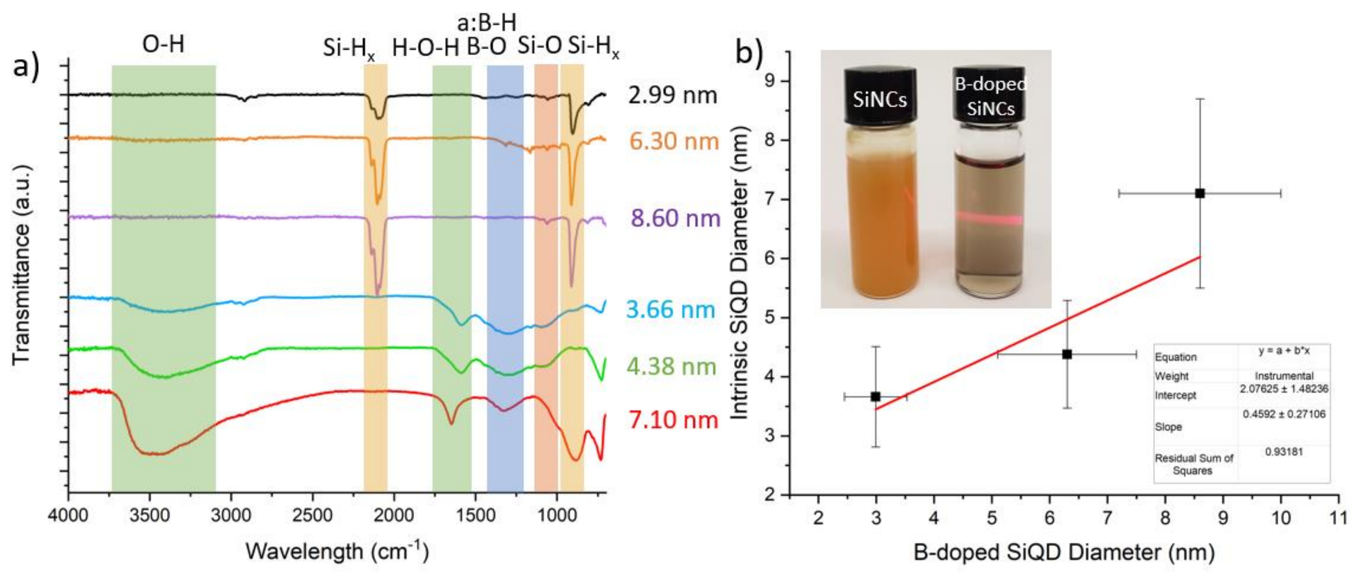

Figure S8 a) Fourier transform infrared spectra (FTIR) for indicated precursor intrinsic SiQDs and corresponding as-synthesized B-doped SiQDs. Particle sizes indicated on the spectra correspond to the d_{TEM} of preformed intrinsic SiQDs (2.99, 6.30 and 8.60 nm) and B-doped SiQDs (3.66, 4.38 and 7.10 nm).

b) Plot of measured d_{TEM} of intrinsic SiQDs vs. B-doped SiQDs. Inset: photograph of suspensions of intrinsic SiQDs (toluene; left) and B-doped SiQDs (ethanol; right). A standard handheld laser pointer is used to show the Tyndall effect of the doped particle mixture.

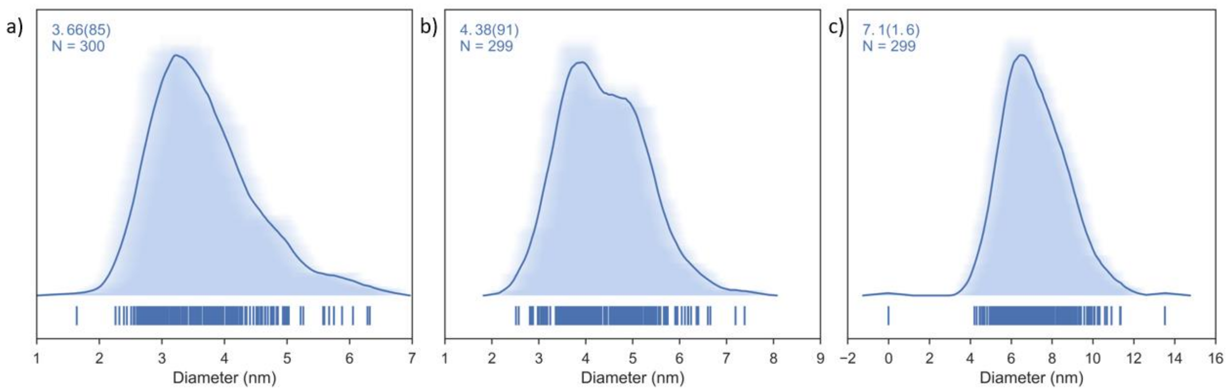

Figure S9 Average shifted histograms obtained from bright field TEM images of B-doped SiQDs produced using precursor SiQDs with TEM determined dimensions of a) 3.66 ± 0.85 nm b) 4.38 ± 0.92 nm and c) 7.10 ± 1.6 nm.

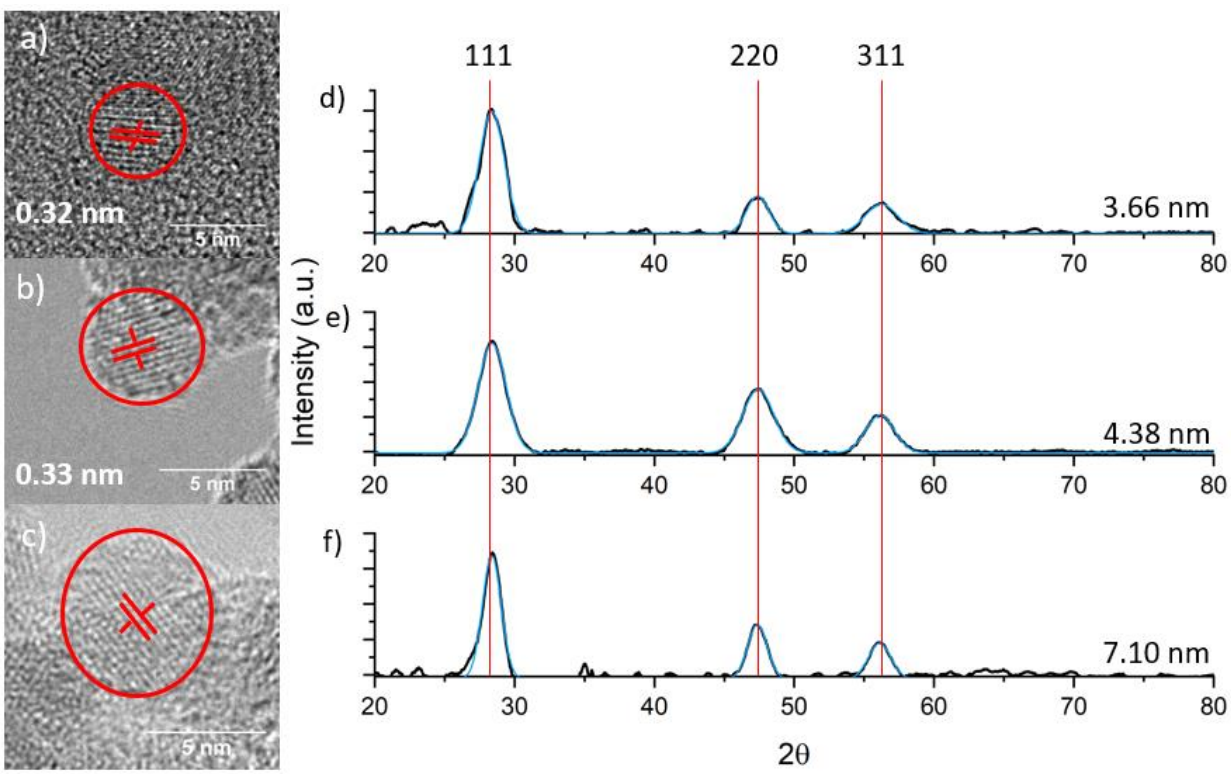

Figure S10 High-resolution TEM of as-synthesized B-doped SiQDs with average TEM determined diameters of a) 3.66 ± 0.85 nm b) 4.38 ± 0.92 nm and c) 7.10 ± 1.6 nm. Powder X-ray diffraction patterns of as-synthesized B-doped SiQDs with diameters of d) 3.66 nm, e) 4.38 nm and f) 7.10 nm. Experimental data is shown as black traces. Blue lines show the Gaussian-Lorentzian multiple-peak fitting.

Table S3 Debye-Scherrer analysis of powder X-ray diffraction patterns collected from B-doped SiQDs of three different sizes: 3.66 ± 0.85 nm, 4.38 ± 0.92 nm and 7.10 ± 1.6 nm.

d_{TEM} = 3.66 nm			d_{TEM} = 4.38 nm			d_{TEM} = 7.10 nm		
Peak position (2θ)	FWHM	Crystallite Size (nm)	Peak position (2θ)	FWHM	Crystallite Size (nm)	Peak position (2θ)	FWHM	Crystallite Size (nm)
28.34	4.00	2.05	28.38	2.11	3.89	28.38	1.581	5.18
47.39	3.98	2.18	47.38	1.88	4.62	47.36	1.63	5.32
55.96	3.78	2.38	56.23	2.74	3.28	56.11	1.87	4.81

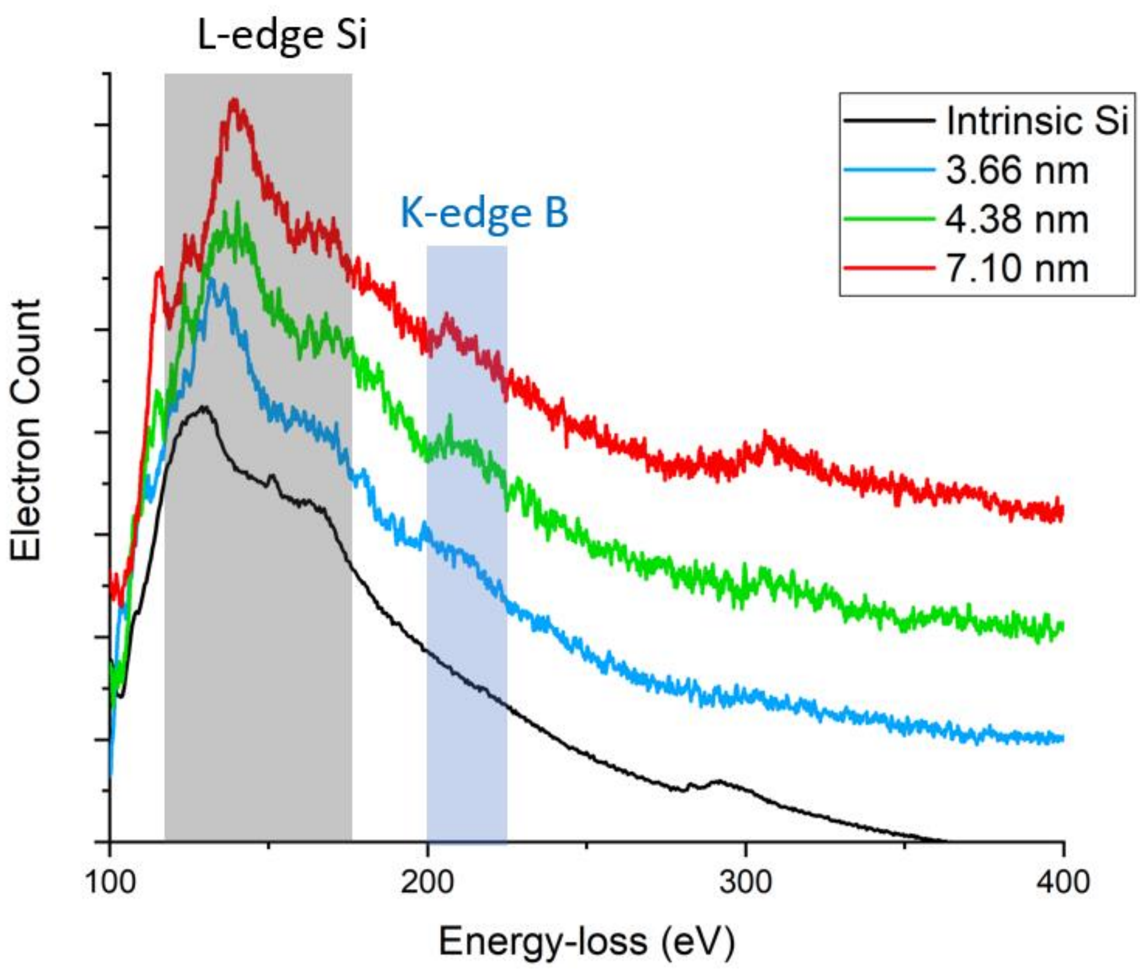

Figure S11 Electron energy-loss spectrum of as-synthesized B-doped SiQDs with average diameter of 3.66 ± 0.85 (blue), 4.38 ± 0.91 (green) and 7.10 ± 1.6 nm (red) compared to intrinsic Si (black).

Table S4 Integrated intensities of the "surface" and "core" B species determined by taking the area under the fitted peaks centred at 188.7 eV and 187.7 eV, respectively, in the B 1s XP spectra for samples with average d_{TEM} dimensions of 3.66, 4.38, and 7.10 nm.

d_{TEM}	Area of "surface" species (188.7 eV)	Area of "core" species (187.7 eV)
3.66	169.5	108.0
4.38	69.7	105.1
7.10	49.9	102.0

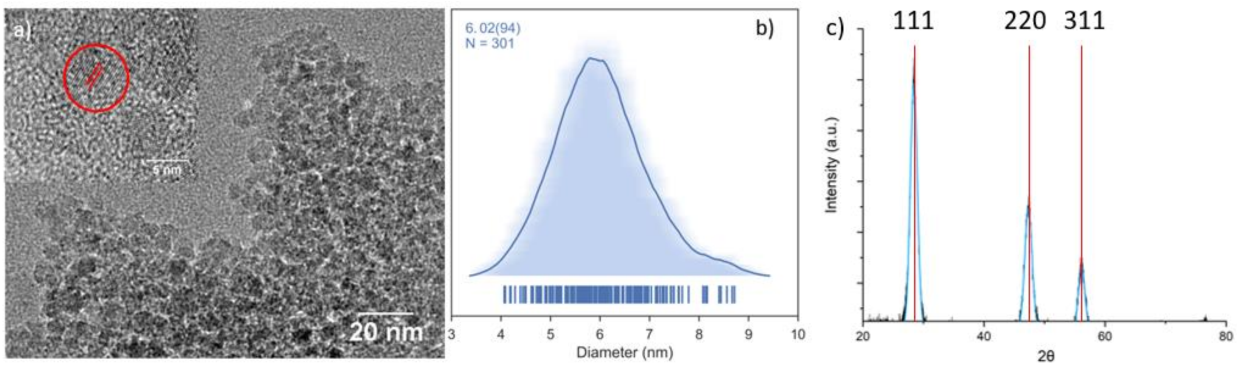

Figure S12 a) Bright field and high-resolution (inset) TEM of 9 nm intrinsic SiQDs that were "over-etched" to 6 nm using ethanolic HF to remove their amorphous shell and b) the corresponding histogram. c) PXRD pattern obtained from a representative over-etched sample showing characteristic reflections from crystalline silicon. Experimental data is shown as black traces. Blue lines show the Gaussian-Lorentzian multiple-peak fitting.

Table S5: Corresponding TEM dimensions and crystallite sizes of precursor SiQDs and B-doped SiQDs determined using the Debye-Scherrer Equation

Precursor SiQD d_{TEM} (nm)	**Precursor SiQD d_{XRD} (nm)**	**B-doped SiQDs d_{TEM} (nm)**	**B-doped SiQDs d_{XRD} (nm)**
2.99	2.11	3.66	2.02
6.30	3.93	4.38	3.63
8.60	6.75	7.10	5.11
6.02	5.74	5.42	4.89

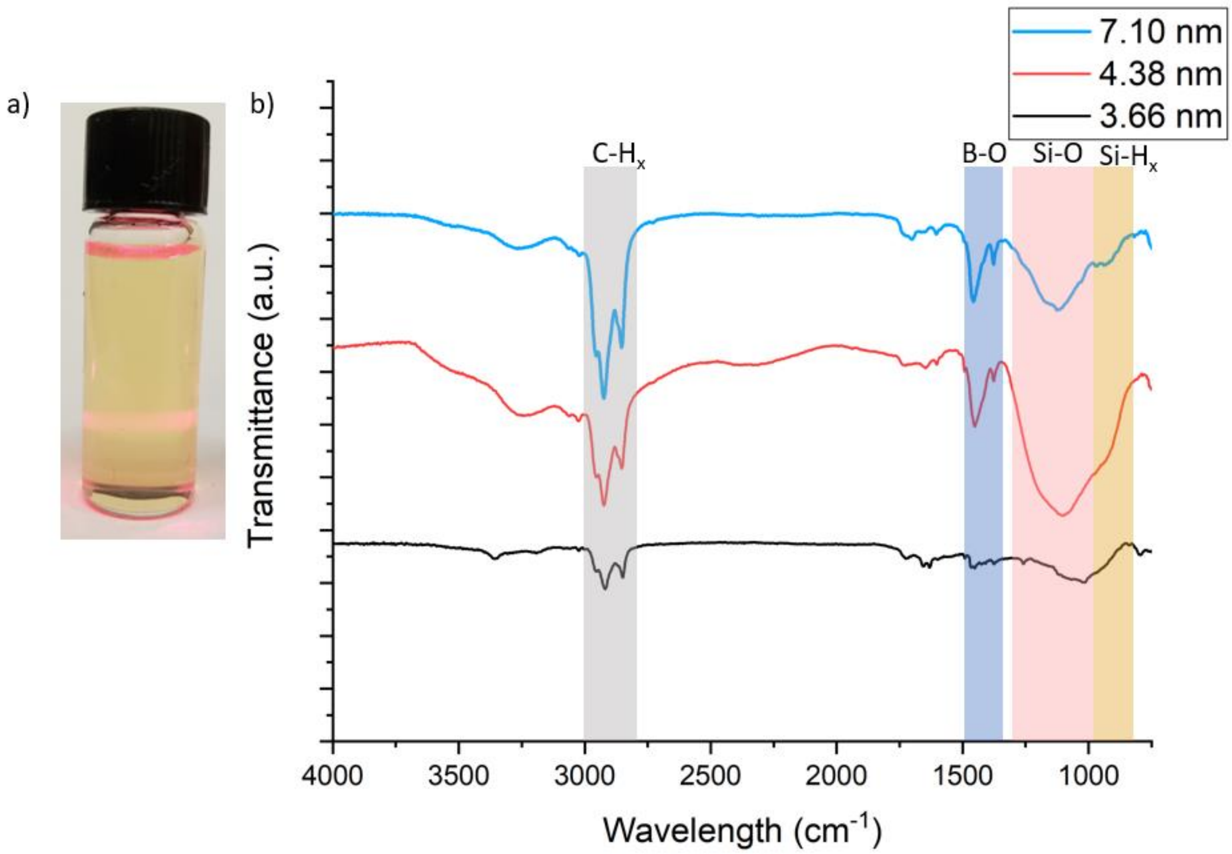

Figure S13 a) A photograph of a toluene suspension of d_{TEM} = 4.38 nm B-doped SiQDs obtained from their reaction with PCl_5 and 1-decanol. The beam of a standard handheld laser pointer is used to show a Tyndall effect. b) FTIR of 1-decylate functionalized B-doped SiQDs for the indicated particle sizes.

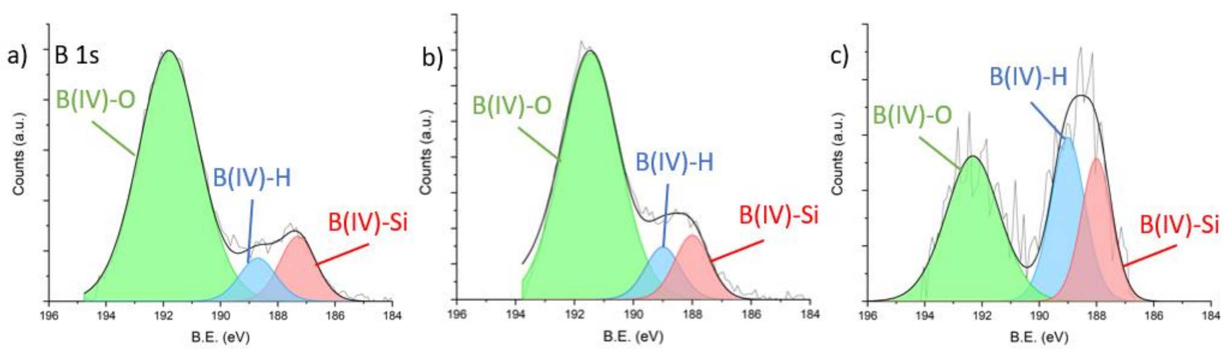

Figure S14 High-resolution XP spectra of B 1s for 1-decylate functionalized B-doped SiQDs with average TEM determined sizes of a) 3.66 nm, b) 4.38 nm and c) 7.10 nm.

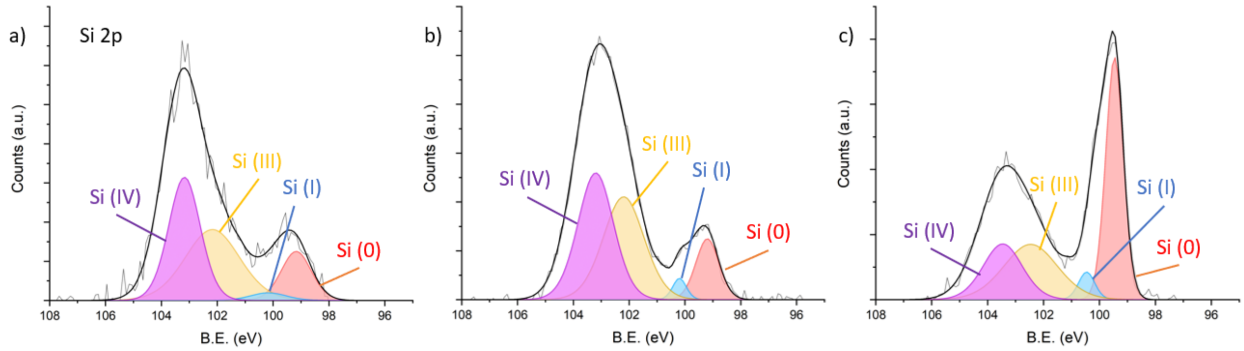

Figure S15 High-resolution XP spectra of Si 2p region for 1-decylate functionalized B-doped SiQDs with TEM determined average sizes of a) 3.66 nm, b) 4.38 nm and c) 7.10 nm.

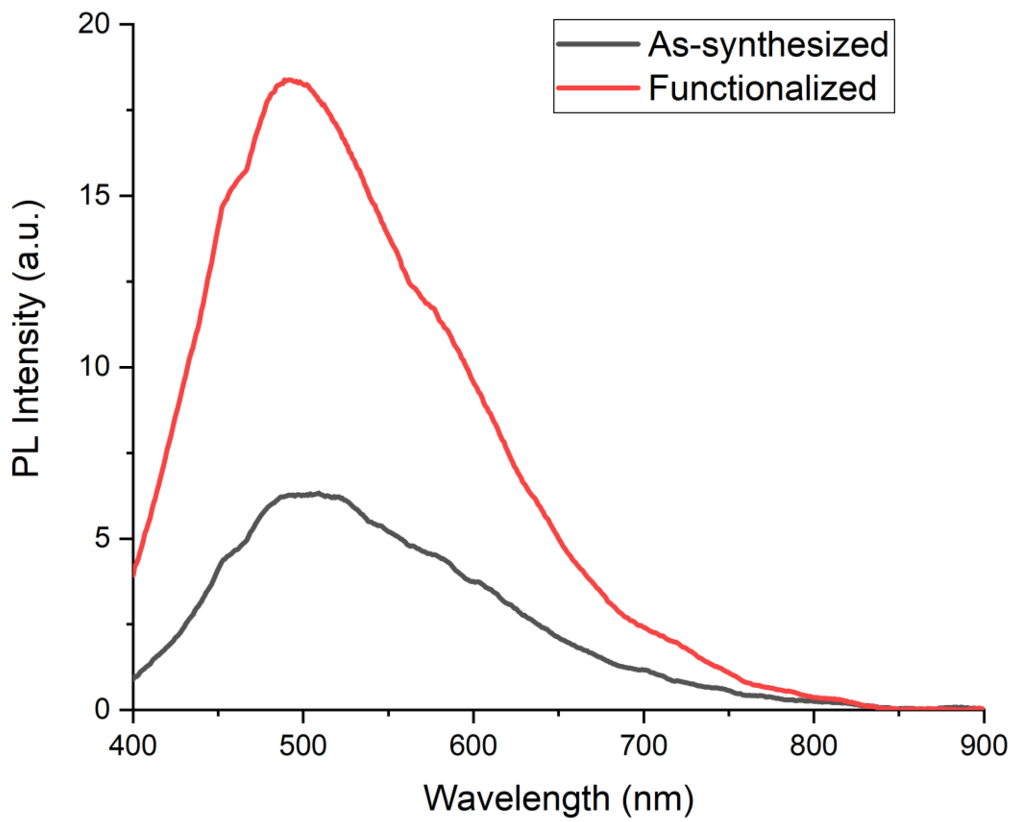

Figure S16 Photoluminescence spectra of B-doped SiQDs with TEM determined average diameters of 3.66 nm before (black) and after functionalization with 1-decanol (red). This data illustrates the impact of functionalization on PL intensity.

Time-dependent emission decay profiles were taken at PL max peak energy for each sample and follow biexponential decay kinetics. The following equation was used to fit the data in Figure S13:

$$f(t) = a_1 e^{-\frac{1}{\tau_1}} + a_2 e^{-\frac{1}{\tau_2}} + b$$

Table S6 PL decay lifetimes of B-doped 1-decylate functionalized SiQDs

Particle d_{TEM}	a_1	τ_1	a_2	τ_2	R^2
3.66 nm	0.8795	4.633	0.05567	120.5	0.9975
4.38 nm	0.5797	38.98	0.4053	141.1	0.9984
7.10 nm	0.4634	153.4	0.5341	489.6	0.9997